Carbohydrate Polymers 98 (2013) 1056–1064

Contents lists available at SciVerse ScienceDirect

Carbohydrate Polymers

journal homepage: www.elsevier.com/locate/carbpol

Synthesis and properties of silane-fluoroacrylate grafted starch

Jia Qu, Ling He*

Department of Chemistry, School of Science, Xi'an Jiaotong University, Xi'an 710049, China

ARTICLE INFO

Article history:
Received 4 February 2013
Received in revised form 4 July 2013
Accepted 7 July 2013
Available online 16 July 2013

Keywords:
Starch
Silane coupling agent
Fluoroacrylate copolymer
Morphology of latex
Surface properties
Thermostability
Mechanical properties

ABSTRACT

The latex of silane-fluoroacrylate grafted starch for coating materials, VTMS-starch/P(MMA/BA/3FMA), is obtained by two step grafting reactions. Vinyltrimethoxysilane (VTMS) is primarily grafted onto starch by condensation between Si—OH and C—OH at 120 °C, and then the copolymer of methyl methacrylate (MMA), butyl acrylate (BA) and 2,2,2-trifluoroethyl methacrylate (3FMA) is grafted onto the VTMS-starch by emulsion polymerization. Fourier transform infrared spectrometry (FTIR) and X-ray photoelectron spectroscopy (XPS) have been used to confirm the chemically grafting reactions in every step. The conversion percent, grafting percent and grafting efficiency for VTMS-starch/p(MMA/BA/3FMA) latex indicate that the optimum conditions should be controlled at 75 °C for 1 h as VTMS-starch/P(MMA/BA/3FMA) in 1/3 weight ratio. Transmission electron microscopy (TEM) and dynamic light scattering (DLS) analysis have revealed that the latexes exhibit the uniform spherical particles of 40–60 nm in a narrow size distribution. The latex films perform the obvious hydrophobic (107°) property, lower surface free energy (25–35 mN/m) and the higher thermostability (330–440 °C) than starch (51°, 51.32 mN/m, 100–330 °C). Dynamic thermomechanical analysis (DMA) shows that the latex film could gain considerable toughness and strength with an elongation at break of 39.45% and a tensile strength of 11.97 MPa.

1. Introduction

Starch is one of the most abundant natural polysaccharide materials, and has been widely used as biodegradable materials (Jiménez, Fabra, Talens, & Chiralt, 2012), binding materials (Okunlola & Odeku, 2011), reinforcing materials (Lemos & Ferreira, 2000; Minatti, Santana, Fernandes, & Campos, 2009), thickener (Teli, Rohera, Sheikh, & Singhal, 2009) and sticky rice–lime mortar in ancient Chinese buildings (Yang, Zhang, & Ma, 2010) because of its renewable, inexpensive, widely available and environmentally friendly properties (Jiménez et al., 2012). However, the poor wet resistance, inferior durability, and weaker mechanical property have severely limited the application of starch as coating materials. Therefore, the modification of starch becomes very necessary in order to overcome its disadvantages and to improve its application. Actively, native starch is composed of two main macromolecular components: amylose and amylopectin (Rindlav-Westling & Gatenholm, 2003). Amylose is a kind of linear polymer of α-1,4 anhydroglucose units, and could form isotropic, odorless, tasteless and colorless film. Amylopectin is a highly branched polymer of short α-1,4 chains linked by α-1,6 glucosidic branching points occurring every 25–30 glucose units. Both amylose and amylopectin are structured by hydrogen bonding (Jiménez et al., 2012). This chemical structure provides the possibility for the modification of starch, such as starch/fumed silica composites (Gun'ko et al., 2008), starch/rubber (Carvalho, Job, Alves, Curvelo, & Gandini, 2003; Rouilly, Rigal, & Gilbert, 2004; Wu, Qi, Liang, & Zhang, 2006) and starch/chitosan (Xu, Kim, Hanna, & Nag, 2005). Chemical reactions like esterification (Angellier, Molina-Boisseau, Belgacem, & Dufresne, 2005; Guan & Hanna, 2004), etherification (Teramoto, Motoyama, Yosomiya, & Shibata, 2003), and conventional polymer grafting have shown the superiority in grafting polymer onto starch. Actually, grafting polymer onto the starch is reported an effective way to overcome the disadvantage of pure starch as coating materials (Meshram, Patil, Mhaske, & Thorat, 2009).

Based on the condition that the fluoroacrylate grafted surface could provide with good thermal and chemical stability, and the excellent film-forming property (Hansen, Jankova, & Hvilsted, 2007; Xiong, Liu, Hong, & Duncan, 2011; Yuan et al., 2011), the well-known fluorine polymer is tried to be grafted onto starch in this paper in order to provide the starch with desired surface properties. Furthermore, the fluoroacrylate copolymer play a significant role in the generation of low-energy surface by self-segregation and self-organization of $-CF_3$ groups in the perfluoroalkyl (Liang, He, Dong, & Zhou, 2012; Ming et al., 2003; Rizzarelli, Rosa, & Torrisi, 2001). Among the various method of introducing the fluoroacrylate copolymer into the hydrocarbon, the typical one is the emulsion polymerization, which could be matched well with the modified

* Corresponding author at: Department of Chemistry, School of Science, Xi'an Jiaotong University, Xianning West Road, 28, Xi'an 710049, China.
Tel.: +86 29 82668554; fax: +86 29 82668559.
E-mail address: heling@mail.xjtu.edu.cn (L. He).

0144-8617/$ – see front matter © 2013 Elsevier Ltd. All rights reserved.
http://dx.doi.org/10.1016/j.carbpol.2013.07.015

starch in aqueous phase, considering the water-soluble property of starch.

In order to facilitate grafting fluoroacrylate onto starch by emulsion polymerization, the silane coupling agents with —CH=CH_2 groups are hoped to serve as the bridge based on the silane grafted coatings with excellent hydrophobicity, resistance to high/low temperature (Kannarpady et al., 2010; Kim, Shin, & Lee, 2007; Rao, Kulkarni, Amalnerkar, & Seth, 2003), and strong adhesion to the substrate (Loch, Ahn, & Chen, 2006; Wang & Schaefer, 2008). But the silane coupling agents of γ-methacryloxypropyltrimethoxysilane (MPS, $H_2C{=}C(CH_3)CO_2(CH_2)_3Si(OCH_3)_3$) and vinyltrimethoxysilane (VTMS, $H_2C{=}CHSi(OCH_3)_3$) are commonly used to modify the inorganic oxides (Gauthier, Aimé, Bouhacina, Attias, & Desbat, 1996; Wang, Mao, Wang, & Fu, 2011; Yu, Xu, & Han, 2011). Little attention is paid to the modification of OH-bearing substances by MPS or VTMS silane agents (Abdelmouleh, Boufi, Salah, Belgacem, & Gandini, 2002; Ly, Belgacem, Bras, & Salon, 2010). Fortunately, the previous hydrolysed alkoxysilane could be firstly physically adsorbed onto the cellulose fibers at room temperature for providing an effective coverage and then chemically grafted after a curing process above 80 °C under an inert atmosphere in order to give a permanent chemical modification of the starch surface (Castellano, Gandini, Fabbri, & Belgacem, 2004), which offers the potential for chemically grafted modification of starch.

This paper presents a new method to prepare the silane-fluoroacrylate grafted starch latex, of VTMS-starch/p(MMA/BA/3FMA) for coating application. VTMS-starch/p(MMA/BA/3FMA) latex is obtained by firstly grafting vinyltrimethoxysilane (VTMS) onto the starch and then grafting poly (methyl methacrylate (MMA)/butyl acrylate (BA)/2,2,2-trifluoroethyl methacrylate(3FMA)) copolymer onto the VTMS-starch. MMA is used as a hard monomer in fluoroacrylate copolymer to increase the hardness of the film, BA as a soft monomer to increase flexibility, and 3FMA as a functional monomer to increase hydrophobicity and lipophobicity. Fourier transform infrared spectrometry (FTIR), X-ray photoelectron spectroscopy (XPS), transmission electron microscopy (TEM), dynamic light scattering (DLS), static contact angle (SCA) and thermogravimetric analysis (TGA) are used for characterizing the chemical structure, morphology and the film properties of VTMS-starch/p(MMA/BA/3FMA) latex.

2. Materials and methods

2.1. Materials

Soluble starch was purchased from Guangdong Guanghua Sci-tech Company, China. It was processed from a kind of potato starch and treated by acid degradation. The molecular weight of purchased starch is about 50,000 and the content of amylose is over 90 wt%. Vinyltrimethoxysilane (VTMS, $H_2C{=}CHSi(OCH_3)_3$, >96 wt%) gained from Silicone New Material Company of Wuhan University was dried over CaH_2 overnight and distilled under reduced pressure. 2,2,2-Trifluoroethyl methacrylate (3FMA, $H_2C{=}C(CH_3)CO_2CH_2CF_3$, 99 wt%) was supplied by Xuejia Company of China. Methyl methacrylate (MMA, 99 wt%) and butyl acrylate (BA, 99 wt%) were supplied by Aldrich, which were rinsed with 5 wt% NaOH aqueous solution and deionized water until the rinsed water reached pH = 7 before using. Ammonium persulfate (APS), alkylphenol ethoxylates (OP-10), sodium dodecyl sulfate (SDS), perfluorooctanesulphonate (PFOS), hydrochloric acid, ethanol, tetrahydrofuran (THF) and chloroform in analytical purity were purchased commercially and were used as received without further purification.

2.2. Methods

2.2.1. Preparation of silane grafted starch

Silane grafted starch was obtained by physical adsorption and chemical grafting. Firstly, the suspension of starch in a mixture of ethanol/water = 80/20 (v/v) and the pre-hydrolyzed VTMS in water/VTMS = 1/1 (molar ratio) at room temperature for 2 h were prepared, separately. The pre-hydrolyzed VTMS was firstly adsorbed onto starch suspension by stirring at pH = 4 for 2 h. Then, the VTMS-adsorbed starch was centrifuged at 2500 rpm for 20 min, vacuum dried at room temperature to remove water and alcohol, and heated at 120 °C under a nitrogen atmosphere for 2 h. After heat treatment, the VTMS chemically grafted starch, VTMS-starch, was obtained by extracting the cured starch in a 24 h Soxhlet with THF in order to remove the non-grafted VTMS. The synthesis of VTMS-starch was shown in Fig. 1.

2.2.2. Preparation of VTMS-starch/p(MMA/BA/3FMA) latex

VTMS-starch (5 wt%) was gelatinized in water at 85 °C for 30 min by the help of a mixed emulsifier of SDS/OP-10/PFOS in a four-mouth-flask equipped with thermometer, stirrer and reflux condenser. $NaHCO_3$ and APS were added into the flask successively after the gelatinized starch was cooled to 70 °C in the water bath. Then, the mixture of MMA, BA and 3FMA in MMA/BA/3FMA = 3/4/3 (w/w) was slowly dripped within 4 h according to the previous research (Zheng, He, Liang, Chang, & Wang, 2011). After this copolymerization was kept for 1 h at 75 °C, VTMS-starch/p(MMA/BA/3FMA) latex was obtained, as shown in Fig. 1. Furthermore, in order to wash off the copolymer of p(MMA/BA/3FMA) in the latex, the obtained latex was precipitated in ethanol, and the dried precipitate was extracted in soxhlet for 36 h by $CHCl_3$.

When the weight ratio of VTMS-starch to P(MMA/BA/3FMA) is varied in 1:1, 1:2, 1:3, 1:4 and 1:5, it indicates that VTMS-starch/P(MMA/BA/TFEMA) in 1:1 and 1:2 give the white latex and crackled films, but 1:3, 1:4 and 1:5 weight ratio present the bluish milky emulsion and flexible translucent films. Therefore, the weight ratio of VTMS-starch to P(MMA/BA/3FMA) should be controlled at least as 1:3 to obtain the desired latex.

2.2.3. Characterization

The chemical structures of VTMS-starch and VTMS-starch/p(MMA/BA/3FMA) latex were characterized using a Tensor 27 FTIR spectrometer of Bruker Optics. Each spectrum was recorded with a resolution of 4 cm^{-1}. Background scans were obtained using the KBr powder. The chemical grafting reactions of VTMS-starch and VTMS-starch/p(MMA/BA/3FMA) latex were also confirmed by X-ray photoelectron spectroscopy (XPS) measurement in an Axis Ultra (England, Kratos Analytical Ltd) using an Al-Ka monochromatic X-ray source (1486.6 eV) operated at 150 W. The overview scans were obtained with energy of 160 eV and acquisition time of 220 s.

The conversion percent (CP) of monomer (the weight ratio of all formed copolymer to monomer taken), grafting percent (GP) (the weight ratio of grafted copolymer to silanized starch taken) and grafting efficiency (GE) of latex (the weight ratio of grafted copolymer to all formed copolymer) were studied by varying the reaction temperature and reaction time. CP, GP and GE were calculated using the following equations:

$$\text{Conversion percent (CP)} = \frac{w_3 - w_2}{w_4} \times 100$$

$$\text{Grafting percent (GP)} = \frac{w_1 - w_2}{w_2} \times 100$$

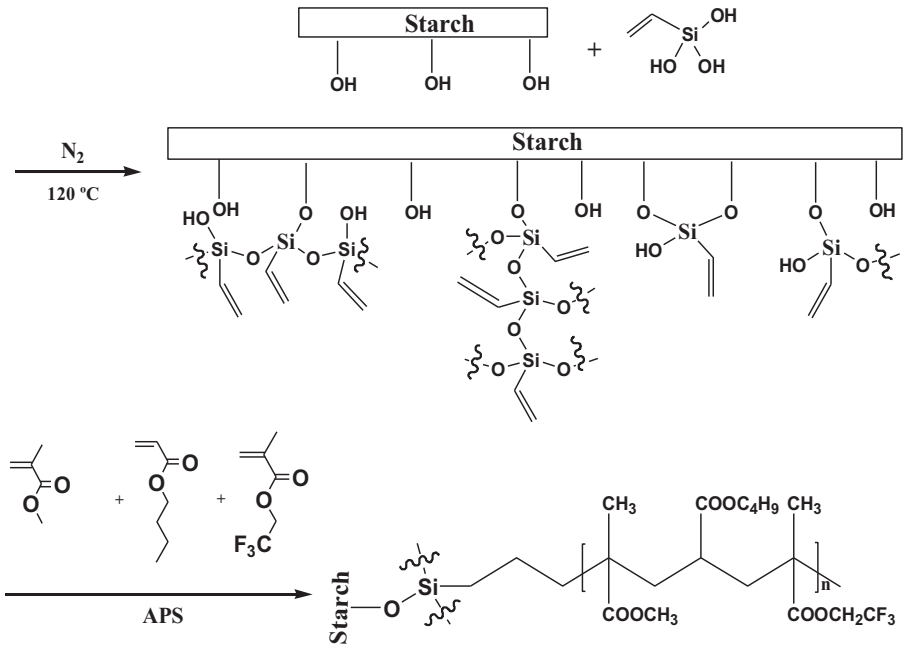

Fig. 1. Reaction scheme of VTMS-starch/p(MMA/BA/3FMA) latex.

$$\text{Grafting efficiency (GE)} = \frac{w_1 - w_2}{w_3 - w_2} \times 100$$

Here, w_1 is the weight of VTMS-starch/p(MMA/BA/3FMA) extracted by $CHCl_3$ (g), w_2 is the weight of VTMS-starch taken (g), w_3 is the weight of precipitate of latex (g), w_4 is the weight of monomer taken (g).

The morphology of VTMS-starch/p(MMA/BA/3FMA) latex was observed with a JEM-200CX transmission electron microscope (TEM) at an acceleration voltage of 120 kV. Samples were prepared by mixing the 50-fold dilutions of original latexes with phosphotungstic acid solution (pH = 2) in 1:1 volume ratio. The aggregates of latex were detected using a MALVERN Nano ZS 90 (Malvern Instruments, UK) dynamic light scattering (DLS) equipped with a He–Ne laser. The scattering data were recorded at 25 ± 0.1 °C in back-scattering mode at a scattering angle of $2\theta = 173°$. The latexes were diluted 50 times and underwent ultrasonic treatment for 5 min before measurement.

The films of VTMS-starch/p(MMA/BA/3FMA) latex were prepared by dropping the latex onto the glass slides to form films at ambient temperature for 72 h. The wettability of films is investigated by the static contact angle (SCA) measurements for both deionized water and hexadecane on the air-exposed film surfaces, which is performed on a JY-82 contact angle goniometer (Hebei Chengde Testing Machine Co. Ltd China) by the sessile drop method with a microsyringe at 25 °C. An average of nine readings of contact angles was used as the final value for each sample. The surface free energy of film surfaces was evaluated by applying the Owens and Wendt method based on static contact angle values. The thermal decomposition of films was obtained using thermogravimetric analysis (TGA), carried out in a nitrogen atmosphere using a NETZSCH TG209 apparatus by heating the sample (each experiment generally involved placing a 10 mg sample on the crucible) from room temperature to 600 °C at a heating rate of 20 °C per minute. The water absorption of the films was obtained by calculation using the water saturated weight (w_2) from entirely immersed in deionized water until equilibrium (24 h) and the initial weight (w_1) as follows:

$$\text{Water absorption}\,\% = \frac{w_2 - w_1}{w_1} \times 100$$

The mechanical property of the latex film was investigated by dynamic thermomechanical analysis (DMA) at a DMA Q800 of TA Instruments, America. The film was cut into 15.4900 mm × 6.9800 mm × 0.0200 mm, equilibrated at 23.00 °C, with a ramp force of 0.0500 N/min to 16.0000 N.

3. Results and discussion

3.1. Synthesis of VTMS-starch/p(MMA/BA/3FMA) latex

FTIR spectra for VTMS-starch and VTMS-starch/p(MMA/BA/3FMA) latex (extracted by $CHCl_3$) are shown in Fig. 2. In order to verify that VTMS is chemical grafted onto starch, VTMS-starch before and after heat treatment are characterized in Fig. 2a and b. From their amplification graphics, the peak at 1415 cm^{-1} for —CH_2— bending and at 1640 cm^{-1} for water adsorbed in the amorphous regions of starch both in Fig. 2a and b are found, but the peak at 1010 cm^{-1} for —Si—OH groups in Fig. 2a is vanished after heating in Fig. 2b, which indicates the condensation between —Si—OH and —C—OH to form —Si—O—C bond in VTMS-starch after heating. However, the C=C absorption comes from VTMS-starch is hardly clarified by FTIR, since the bending vibration of C=C just presents at the location of bending peak for —CH_2— groups in the starch around 1415 cm^{-1}, and the stretching vibration of C=C is just located at the water adsorbed starch around 1640 cm^{-1} of the amorphous regions. Fortunately, the considerable silicon content measured by XPS is able to further prove the graft of VTMS to starch, as shown in Fig. 3 and Table 1, and the supporting information for ^{1}H NMR analysis is able to prove the C—OH bond in starch, Si—OH bond in VTMS and double bond in VTMS (see supporting information S1).

Supplementary data related to this article found, in the online version, at http://dx.doi.org/10.1016/j.carbpol.2013.07.015.

Furthermore, compared with the spectra of VTMS-starch in Fig. 2b, the p(MMA/BA/3FMA) in Fig. 2c, and the FTIR spectrum of VTMS-starch/p(MMA/BA/3FMA) (extracted by $CHCl_3$ for 36 h in order to wash off the non-grafted copolymer) in Fig. 2d, it is found that the characteristic absorptions of C=O at 1740 cm^{-1} and C—F at 1280 cm^{-1} reveal the successful grafting of P(MMA/BA/3FMA)

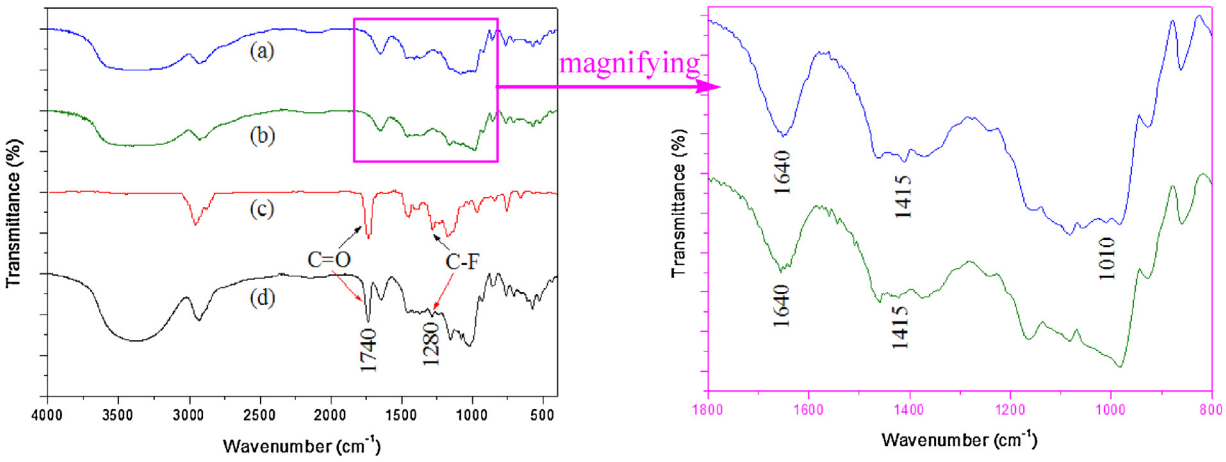

Fig. 2. FTIR spectra of VTMS-starch (a) before and (b) after heat treatment, p(MMA/BA/3FMA) copolymer (c) and VTMS-starch/p(MMA/BA/3FMA) (d).

onto VTMS-starch in Fig. 2d. However, it is difficult to observe Si—O—C absorption peak in Fig. 2d due to the strong absorption of C—O in starch. While, the XPS pattern and the atomic compositions in Fig. 3 and Table 1 are able to further prove the formation of VTMS-starch/p(MMA/BA/3FMA).

Fig. 3 is the XPS patterns of starch, VTMS-starch, VTMS-starch/p(MMA/BA/3FMA) latex and the extracted latex by $CHCl_3$. Compared with the XPS patterns of starch in Fig. 3a, the low-resolution XPS patterns for VTMS-starch in Fig. 3c (the non-grafted VTMS has been washed off by THF) could confirm that the VTMS has been chemical grafted onto the starch by the presence of silicon atoms witnessed at the corresponding peaks of 100 and 150 eV. In order to further verify this grafting reaction, the atom compositions varying with the molar ratio of VTMS to —OH groups in starch as 1:3, 1:1 and 3:1 are determined in Table 1. 15.81–17.46% silicon composition reveals the presence of silicon atoms and therefore the chemical grafting of VTMS onto the starch. While, 15.81–17.46% silicon content in the three VTMS-starch samples indicates that the silicon atom composition are not always increased with the increase of VTMS amount, because there must be the equilibration for the adsorption of VTMS to starch. Therefore, a 1:3 molar ratio is selected in the next polymerization for the effective matching the less VTMS content to more —OH groups. Furthermore, both the XPS patterns of VTMS-starch/p(MMA/BA/3FMA) latex in Fig. 3e and the extracted latex by $CHCl_3$ in Fig. 3g reveal clearly the presence of fluorine and silicon atoms, which confirms the formation of VTMS-starch/p(MMA/BA/3FMA). Although 0.69% silicon content for extracted VTMS-starch/p(MMA/BA/3FMA) latex in Fig. 3g is much less than 3.84% for unextracted latex due to the hydrolysable group of Si—O—C, the obvious fluorine content in Table 1 for 8.24% and 5.38% could confirm the formation of VTMS-starch/p(MMA/BA/3FMA) latex.

For the high-resolution XPS patterns of starch (Fig. 3b), VTMS-starch (Fig. 3d) and VTMS-starch/p(MMA/BA/3FMA) latex before (Fig. 3f) and after extraction (Fig. 3h), the relative percentage of C—C, C—O, O—C=O and C—F is listed in Table 1, respectively. It could be found that the percentage of C—O in VTMS-starch/p(MMA/BA/3FMA) is increased after extraction because the non-grafted copolymer without C—O has been washed off, but the percentage of C—F in VTMS-starch/p(MMA/BA/3FMA) is decreased after extraction due to the washing away of the non-grafted copolymer with higher content of C—F. On the other hand, the percentage content of O—C=O goes a little higher because C—C decreases obviously after extraction.

In this paper, the percentage of the different acrylate monomers introduced into the final latex is not determined, but the total involved acrylate copolymer as a whole is studied. As the polymerization time and temperature affect much on the grafting reaction, CP, GP and GE are therefore discussed in Fig. 4. When the temperature is varied in 70–90 °C, CP, GP and GE are increased and then subsequent decreased (Fig. 4a). CP leads to require the maximum at 75–85 °C, but GP and GE keeps relatively unchanged between 80 °C and 90 °C because of the decomposition of grafted and non-grafted copolymer at high temperature, but the maximum of GP and GE are obtained at 75 °C. Therefore, APS is more easily to initiate VTMS-modified starch at higher temperature, but the diffusion rate of monomer to starch is also quickened at higher temperature, this might be realized by GP of 3.2% at 70 °C, 35.2% at 75 °C and 14.4% at 80 °C. It is worth noticing that the formation of non-grafted polymer is increased obviously when the temperature is over 75 °C. As for the effect of the polymerization time on the latex, Fig. 4b shows that CP increases with time within 40 min, but keeps constant after 1 h. Although the average rising of GP with time is much more than GE because the concentration of mixture monomers and initiator decrease with time and the reaction equilibrium reaches as the reaction progresses, GP and GE could reach their maximum in 1 h. Therefore, the reaction time should be kept not more than 1 h.

Table 1
Element composition of starch, VTMS-starch and VTMS-starch/p(MMA/BA/3FMA).

Samples	Low-resolution XPS				High-resolution XPS			
	%C	%O	%Si	%F	C—C	C—O	O—C=O	C—F
Starch	59.02	40.98	–	–	16.20	83.80	–	–
VTMS-starch (1:3)	50.65	32.93	16.41	–	77.79	22.21	–	–
VTMS-starch (1:1)	50.91	31.63	17.46	–	–	–	–	–
VTMS-starch (3:1)	49.71	34.48	15.81	–	–	–	–	–
VTMS-starch/p(MMA/BA/3FMA) latex	61.10	26.82	3.84	8.24	69.00	20.70	8.34	1.96
VTMS-starch/p(MMA/BA/3FMA) (extracted by $CHCl_3$)	66.34	27.60	0.69	5.38	41.77	42.62	14.40	1.21

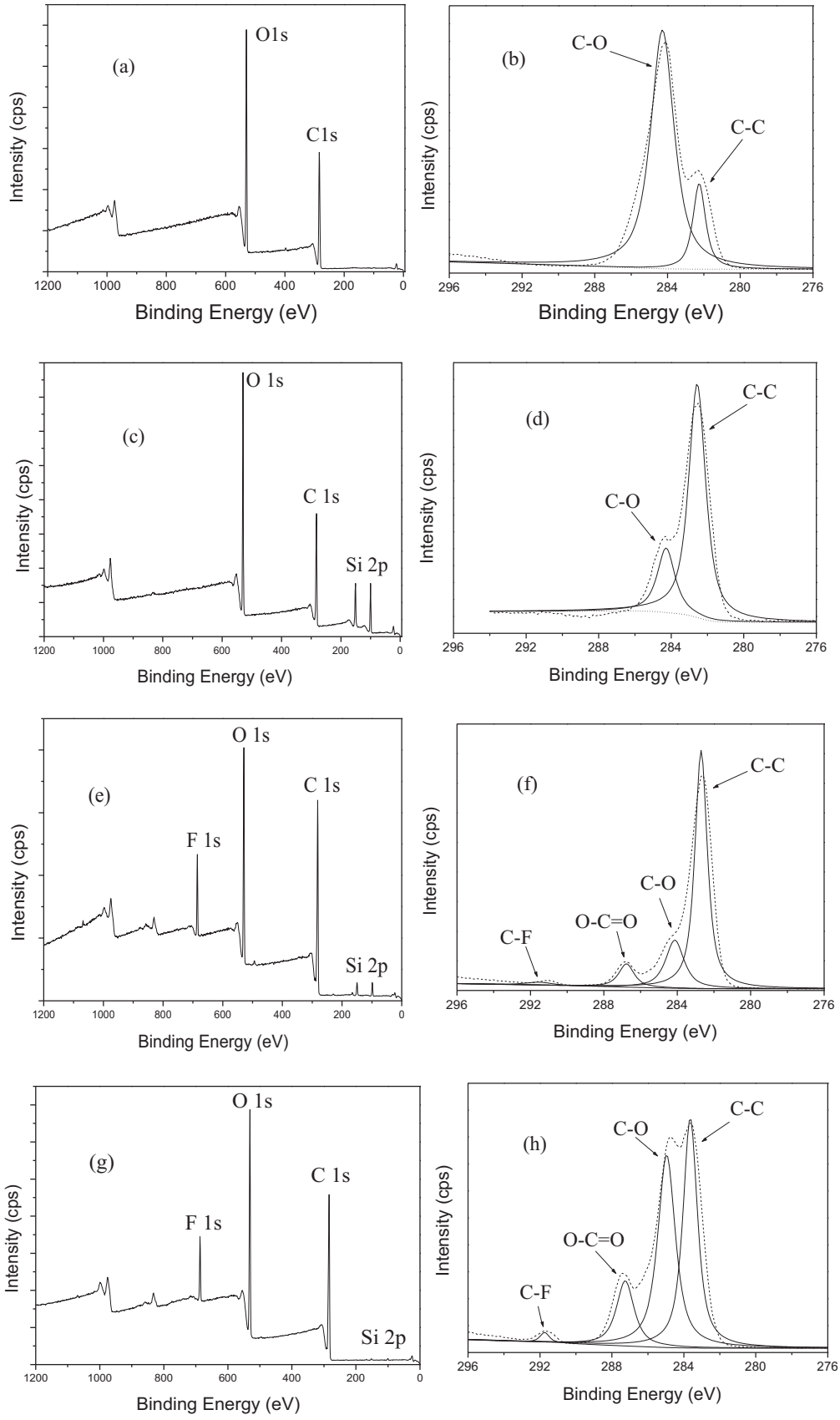

Fig. 3. XPS patterns of starch (a, b), VTMS-starch (c, d), VTMS-starch/p(MMA/BA/3FMA) latex (e, f) and the latex extracted in $CHCl_3$ (g, h).

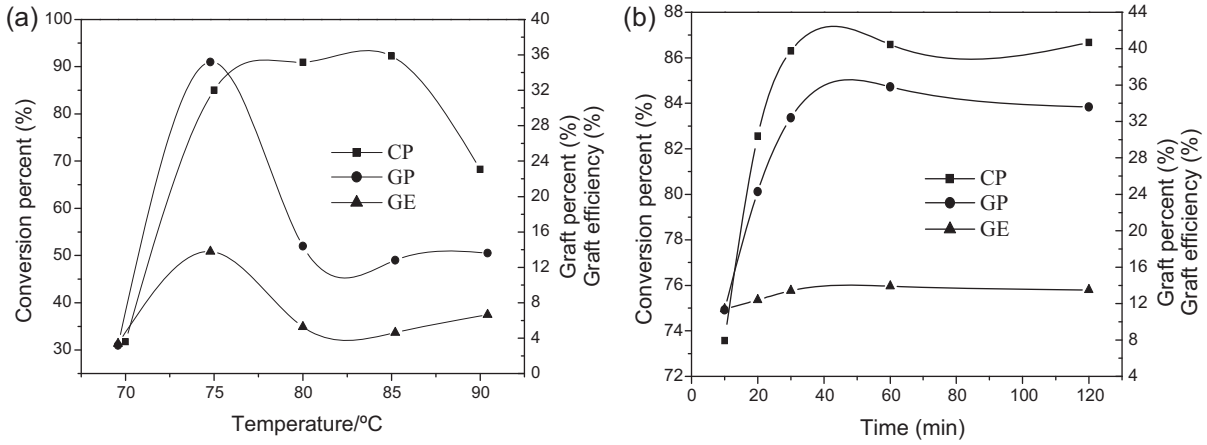

Fig. 4. Effect of reaction temperature (a) and time (b) on the conversion percent, grafting percent and grafting efficiency.

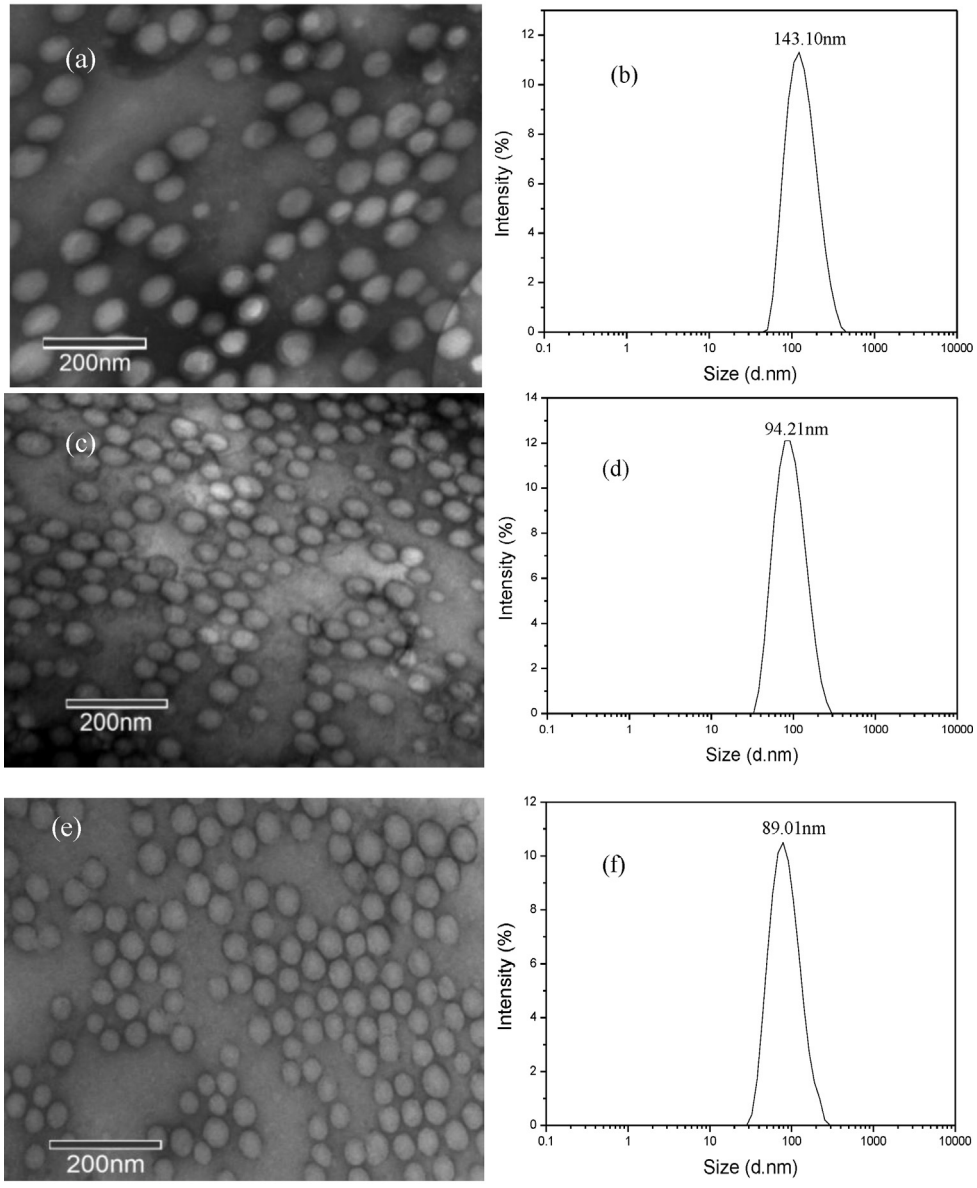

Fig. 5. TEM images and DLS curves of the latexes for Sample 1 (a, b), Sample 2 (c, d) and Sample 3 (e, f).

Table 2
The effect of emulsifier content on the static contact angles, surface free energy and water absorption of VTMS-starch/p(MMA/BA/3FMA) films.

Sample	OP-10/SDS/PFOS (w/w)	θ_{water} (°)	θ_{cetane} (°)	γ_s^d (mN/m)	γ_s^p (mN/m)	γ_s (mN/m)	Water absorption (wt%)
Pure starch	–	51.0	0	27.60	23.72	51.32	45
1	2.0/1.0/0.1	107.0	25.0	25.08	0.11	25.19	n.d.
2	3.3/1.7/0.1	90.3	25.3	25.02	3.24	28.26	n.d.
3	5.3/2.7/0.1	73.8	25.3	25.02	10.56	35.58	n.d.
4	8.0/4.0/0.1	54.0	12.7	26.93	22.09	49.02	n.d.

3.2. Morphologies and size distribution of VTMS-starch/p(MMA/BA/3FMA) latex

The morphologies and particle size distribution of VTMS-starch/p(MMA/BA/3FMA) latex are characterized by TEM observation and DLS measurements, as shown in Fig. 5. The latexes exhibit the uniform spherical particles and narrow particles size distributions in different amount of emulsifier. Comparatively, Fig. 5 indicates that the high emulsifier content gives the smaller particle size of latex and the better particles distribution. For Sample 1 obtained by emulsifier OP-10/SDS/PFOS = 2.0/1.0/0.1, the latex particles exhibits a binomial distribution with the larger particles in average diameter of 50–60 nm and a little of smaller particles of 20 nm (Fig. 5a). But with the increase of emulsifier content into OP-10/SDS/PFOS = 3.3/1.7/0.1 (Fig. 5c, Sample 2) and 5.3/2.7/0.1 (Fig. 5e, Sample 3), the latex particles show a very uniform morphology, especially in Fig. 5e for Sample 3, and Sample 4 is actually very similar to Sample 3. Fig. 5 reveals that the higher emulsifier content benefits to the homogenous and smaller particles because the particles of latex in Fig. 5e (40 nm) is a little smaller than the latex in Fig. 5c (50 nm) and Fig. 5a (50–60 nm), which has been proved by Fowler et al. (2011). On the other hand, the narrow partial size distribution of latex is verified by the unimodal distribution of DLS curves in Fig. 5. For Sample 1 (Fig. 5b), Sample 2 (Fig. 5d) and Sample 3 (Fig. 5f), the particles sizes are 143.1 nm, 94.2 nm and 89.0 nm, respectively, which indicates that the diameter of latexes particle observed in TEM is much smaller than in DLS curves. The reason may be that both analysis of TEM and DLS are in the different sample states. DLS analysis is measured in dilute latexes, which the particles might be surrounded by emulsifiers, water molecules and other substances, while TEM images are measured in films.

3.3. The wettability and surface free energy of VTMS-starch/p(MMA/BA/3FMA) film

Table 2 gives the static contact angle (SCA) and the calculated surface free energy of different films obtained by VTMS-starch/p(MMA/BA/3FMA) latexes. It is clear to see that the water contact angles of VTMS-starch/p(MMA/BA/3FMA) films (Sample 1–3, 73.8–107°) is obviously enhanced compared with starch film (51°), and therefore the corresponding surface free energy (25.19–35.58 mN/m) is lower than that for the starch film (51.32 mN/m), which is attributed to the grafting of fluorosilicone copolymer onto starch. However, when the emulsifier content of OP-10/SDS/PFOS is controlled as 2.0/1.0/0.1, 3.3/1.7/0.1 and 5.3/2.7/0.1, the water contact angles of films decrease correspondingly (107.0°, 90.3° and 73.8°, separately) because of the accumulation of emulsifier on the film surface, but the cetane contact angles remain constant as 25.0–25.3°, which lend to a increasing of surface free energy of films for Sample 1–3 as 25.19–35.58 mN/m. When OP-10/SDS/PFOS is controlled as 8.0/4.0/0.1 in Sample 4, both the water contact angle (54.0°) and the cetane contact angle (12.7°) are decreased by much content of OP-10/SDS, and therefore the surface free energy (49.02 mN/m) is increased. Furthermore, the comparison of water absorption between the starch film and the latex films (Samples 1–4) indicates that the starch gives 45% water absorption, but the latex films give almost no water absorption due to the involvement of fluorosilicone copolymer. Therefore, the modified films have excellent water resistance as coating materials.

3.4. The thermostability of VTMS-starch/p(MMA/BA/3FMA)

The thermostability of VTMS-starch/p(MMA/BA/3FMA) is investigated by TGA with the thermal degradability in the temperature range of 25–600 °C, as is shown in Fig. 6. Pure starch, p(MMA/BA/3FMA) copolymer and VTMS-starch/p(MMA/BA/3FMA) (extracted by $CHCl_3$) are investigated under a nitrogen atmosphere, while VTMS-starch/p(MMA/BA/3FMA) (extracted by $CHCl_3$) is additionally analyzed under an air atmosphere. For the starch, Fig. 6 shows that the weight loss of pure starch from room temperature to 120 °C is only 16.1% due to the evaporation of absorbed water, but starch starts to decompose from 120 °C to 290 °C until it is totally decomposed from 290 °C to 320 °C, and finally tends to smooth above 320 °C with 13.5% residual carbon. While, the TG curve for p(MMA/BA/3FMA) copolymer shows only one step of decomposition under the nitrogen atmosphere as starting to decompose at 350 °C and decomposes totally at 430 °C, which indicates the good thermostability of p(MMA/BA/3FMA) copolymer. However, comparing with the pure starch and p(MMA/BA/3FMA) copolymer, it is found that the degradation process of VTMS-starch/p(MMA/BA/3FMA) is composed of three steps. The first step starts from room temperature to 120 °C with the weight loss about 9.1% due to the evaporation of absorbed water, the second step from 300 °C to 320 °C is due to the decomposition of starch, and the third step from 320 °C to 430 °C slows down with a new degradation process. This new degradation process is attributed to the grafting of p(MMA/BA/3FMA) into VTMS-starch, which has also been proved by the TG curve of VTMS-starch/p(MMA/BA/3FMA) under an air atmosphere, because

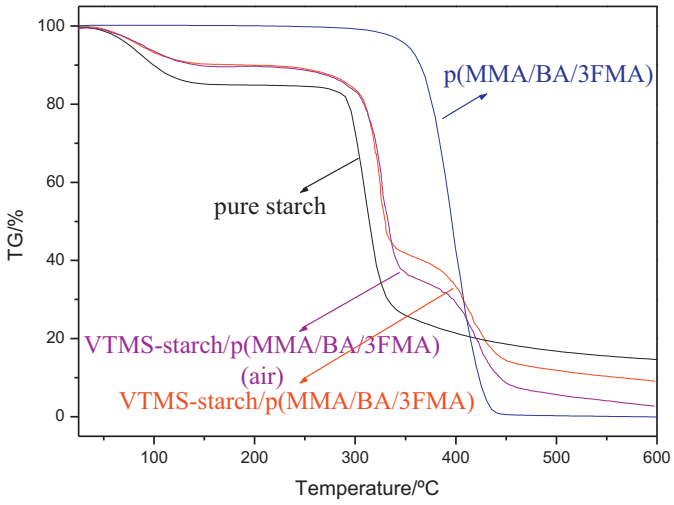

Fig. 6. TGA curves of VTMS-starch/p(MMA/BA/3FMA), p(MMA/BA/3FMA) and starch under nitrogen atmosphere and VTMS-starch/p(MMA/BA/3FMA) alone under air atmosphere.

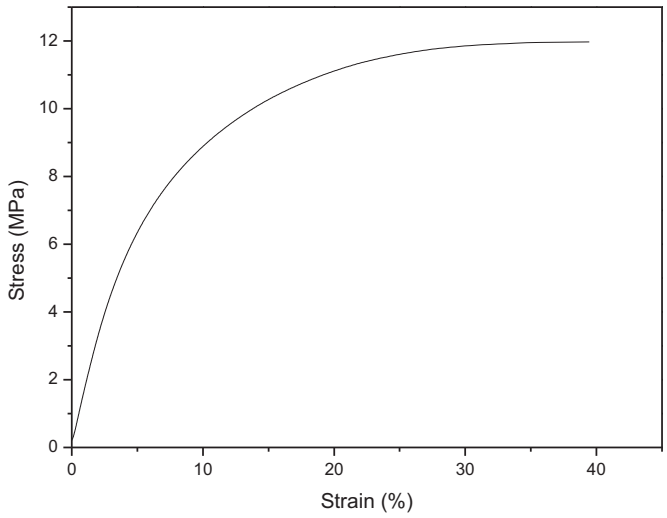

Fig. 7. The stress-strain curve of VTMS-starch/p(MMA/BA/3FMA) film.

the residual carbon and silicon of VTMS-starch/p(MMA/BA/3FMA) under a nitrogen atmosphere is about 9.1%, and the residual silicon (namely silica) under an air atmosphere is about 2.7%. These results prove that VTMS-starch/p(MMA/BA/3FMA) latex is able to suggest as the thermostable coating material.

3.5. The mechanical properties of the latex film

The mechanical properties of the VTMS-starch/p(MMA/BA/3FMA) latex film is investigated by DMA, and the stress–strain curve of the latex film is shown in Fig. 7. The film shows considerable toughness with an elongation at break of 39.45% and a tensile strength of 11.97 MPa. The Young's modulus of this film is about 160 MPa, which reveals the ability of anti-elastic deformation of VTMS-starch/p(MMA/BA/3FMA) film. Since the native starch film is too brittle to be tested, it is impossible to compare the obtained results with the native starch. Here, in order to illustrate the improvement of mechanical properties in modified starch of VTMS-starch/p(MMA/BA/3FMA) film, the literature by Lili Ren et al. (2010) for the influences of starch modification using dodecenyl succinic anhydride (DDSA) and octenyl succinic anhydride (OSA) on the mechanical properties of native starch films is used for the comparison. The tensile strength of DDSA treated and OSA treated films are (9.70 ± 1.11) MPa and (5.36 ± 0.55) MPa, the Young's modulus of DDSA treated and OSA treated films are (152.77 ± 18.28) MPa and (70.88 ± 4.92) MPa, the elongation at break of DDSA treated and OSA treated films are (22.97 ± 3.00)% and (54.45 ± 3.61)%. Therefore, it is possible to sure that the mechanical properties for the film obtained from VTMS-starch/p(MMA/BA/3FMA) latex is improved greatly by the grafting modification.

4. Conclusions

In this paper, we report the preparation of the environmental friendly coating material of vinyltrimethoxysilane and poly (methyl methacrylate/butyl acrylate and 2,2,2-trifluoroethyl methacrylate) grafted starch, VTMS-starch/p(MMA/BA/3FMA) latex, and the property of latex and films. The silane coupling agent of VTMS is primarily adsorbed physically at room temperature and then chemically grafted at high temperature onto the starch. But the fluoroacrylate copolymer p(MMA/BA/3FMA) is grafted on to VTMS-starch by emulsion polymerization at the help of emulsifier OP-10/SDS/PFOS. When MMA/BA/TFEMA = 3/4/3 (w/w) and the mole ratio of VTMS-starch to P(MMA/BA/TFEMA) = 1/3, the obtained latexes are distributed in the average diameter of 40–50 nm with the uniform spherical particles and the narrow particles size distributions. Compared with the starch film (51.0° water contact angle, 51.32 mN/m surface free energy), VTMS-starch/p(MMA/BA/3FMA) films exhibit the excellent hydrophobicity (107° water contact angle) and lipophobicity (25.0° cetane contact angle), the lower surface free energy (25.19 mN/m), and the higher thermostability (330–440 °C). The mechanical properties of the VTMS-starch/p(MMA/BA/3FMA) latex film is improved greatly by the modification as to considerable toughness with an elongation at break of 39.45% and a tensile strength of 11.97 MPa. These results suggest that VTMS-starch/p(MMA/BA/3FMA) latex is expected to be the hydrophobic, thermostable and tough coating material.

Acknowledgements

This work has been financially supported by the National Basic Research Program of China (973 Program, no. 2012CB720904), by the National Natural Science Foundation of China (NSFC grants no. 51073126) and by the State Administration of Cultural Heritage (20110128). The authors also wish to express their gratitude for the MOE Key Laboratory for Non-equilibrium Condensed Matter and Quantum Engineering of Xi'an Jiaotong University.

References

Abdelmouleh, M., Boufi, S., Salah, A., Belgacem, M. N., & Gandini, A. (2002). Interaction of silane coupling agents with cellulose. *Langmuir*, *18*, 3203–3208.
Angellier, H., Molina-Boisseau, S., Belgacem, M. N., & Dufresne, A. (2005). Surface chemical modification of waxy maize starch nanocrystals. *Langmuir*, *21*, 2425–2433.
Carvalho, A. J. F., Job, A. E., Alves, N., Curvelo, A. A. S., & Gandini, A. (2003). Thermoplastic starch/natural rubber blends. *Carbohydrate Polymers*, *53*, 95–99.
Castellano, M., Gandini, A., Fabbri, P., & Belgacem, M. N. (2004). Modification of cellulose fibres with organosilanes: Under what conditions does coupling occur? *Journal of Colloid and Interface Science*, *273*, 505–511.
Fowler, C. I., Muchemu, C. M., Miller, R. E., Phan, L., O'Neill, C., Jessop, P. G., et al. (2011). Emulsion polymerization of styrene and methyl methacrylate using cationic switchable surfactants. *Macromolecules*, *44*, 2501–2509.
Gauthier, S., Aimé, J. P., Bouhacina, T., Attias, A. J., & Desbat, B. (1996). Study of grafted silane molecules on silica surface with an atomic force microscope. *Langmuir*, *12*, 5126–5137.
Guan, J., & Hanna, M. A. (2004). Extruding foams from corn starch acetate and native corn starch. *Biomacromolecules*, *5*, 2329–2339.
Gun'ko, V. M., Pissis, P., Spanoudaki, A., Turova, A. A., Turov, V. V., Zarko, V. I., et al. (2008). Interfacial phenomena in starch/fumed silica at varied hydration levels. *Colloids and Surfaces A: Physicochemical and Engineering Aspects*, *320*, 247–259.
Hansen, N. M. L., Jankova, K., & Hvilsted, S. (2007). Fluoropolymer materials and architectures prepared by controlled radical polymerizations. *European Polymer Journal*, *43*, 255–293.
Jiménez, A., Fabra, M. J., Talens, P., & Chiralt, A. (2012). Edible and biodegradable starch films: A review. *Food and Bioprocess Technology*, *5*, 2058–2076.
Kannarpady, G. K., Sharma, R., Liu, B., Trigwell, S., Ryerson, C., & Biris, A. S. (2010). Silane decorated metallic nanorods for hydrophobic applications. *Applied Surface Science*, *256*, 1679–1682.
Kim, N., Shin, D. H., & Lee, Y. T. (2007). Effect of silane coupling agents on the performance of RO membranes. *Journal of Membrane Science*, *300*, 224–231.
Lemos, A. F., & Ferreira, J. M. F. (2000). Porous bioactive calcium carbonate implants processed by starch consolidation. *Materials Science and Engineering C*, *11*, 35–40.
Liang, J., He, L., Dong, X., & Zhou, T. (2012). Surface self-segregation, wettability, and adsorption behavior of core–shell and pentablock fluorosilicone acrylate copolymers. *Journal of Colloid and Interface Science*, *369*, 435–441.
Lili Ren, L., Jiang, M., Tong, J., Bai, X., Dong, X., & Zhou, J. (2010). Influence of surface esterification with alkenyl succinic anhydrides on mechanical properties of corn starch films. *Carbohydrate Polymers*, *82*, 1010–1013.
Loch, C. L., Ahn, D., & Chen, Z. (2006). Sum frequency generation vibrational spectroscopic studies on a silane adhesion-promoting mixture at a polymer interface. *Journal of Physical Chemistry B*, *110*, 914–918.
Ly, B., Belgacem, M. N., Bras, J., & Salon, M. C. B. (2010). Grafting of cellulose by fluorine-bearing silane coupling agents. *Materials Science and Engineering C*, *30*, 343–347.
Meshram, M. W., Patil, V. V., Mhaske, S. T., & Thorat, B. N. (2009). Graft copolymers of starch and its application in textiles. *Carbohydrate Polymers*, *75*, 71–78.

Minatti, J. L., Santana, J. G. A., Fernandes, R. S., & Campos, E. (2009). Alumina developed by pre-gelling starch consolidation (PSC). *Journal of the European Ceramic Society*, *29*, 661–668.

Ming, W., Melis, F., Grampel, R. D., Ravenstein, L., Tian, M., & Linde, R. (2003). Low surface energy films based on partially fluorinated isocyanates: The effects of curing temperature. *Progress in Organic Coatings*, *48*, 316–321.

Okunlola, A., & Odeku, O. A. (2011). Evaluation of starches obtained from four Dioscorea species as binding agent in chloroquine phosphate tablet formulations. *Saudi Pharmaceutical Journal*, *19*, 95–105.

Rao, A. V., Kulkarni, M. M., Amalnerkar, D. P., & Seth, T. (2003). Surface chemical modification of silica aerogels using various alkyl-alkoxy/chloro silanes. *Applied Surface Science*, *206*, 262–270.

Rindlav-Westling, A., & Gatenholm, P. (2003). Surface composition and morphology of starch, amylose, and amylopectin films. *Biomacromolecules*, *4*, 166–172.

Rizzarelli, P., Rosa, C. L., & Torrisi, A. (2001). Testing a fluorinated compound as a protective material for calcarenite. *Journal of Cultural Heritage*, *2*, 55–62.

Rouilly, A., Rigal, L., & Gilbert, R. G. (2004). Synthesis and properties of composites of starch and chemically modified natural rubber. *Polymer*, *45*, 7813–7820.

Teli, M. D., Rohera, P., Sheikh, J., & Singhal, R. (2009). Application of germinated maize starch in textile printing. *Carbohydrate Polymers*, *75*, 599–603.

Teramoto, N., Motoyama, T., Yosomiya, R., & Shibata, M. (2003). Synthesis, thermal properties, and biodegradability of propyl-etherified starch. *European Polymer Journal*, *39*, 255–261.

Wang, C., Mao, H., Wang, C., & Fu, S. (2011). Dispersibility and hydrophobicity analysis of titanium dioxide nanoparticles grafted with silane coupling agent. *Industrial and Engineering Chemistry Research*, *50*, 11930–11934.

Wang, P., & Schaefer, D. W. (2008). Why does silane enhance the protective properties of epoxy films? *Langmuir*, *24*, 13496–13501.

Wu, Y., Qi, Q., Liang, G., & Zhang, L. (2006). A strategy to prepare high performance starch/rubber composites: In situ modification during latex compounding process. *Carbohydrate Polymers*, *65*, 109–113.

Xiong, D., Liu, G., Hong, L., & Duncan, E. J. S. (2011). Superamphiphobic diblock copolymer coatings. *Chemistry of Materials*, *23*, 4357–4366.

Xu, Y. X., Kim, K. M., Hanna, M. A., & Nag, D. (2005). Chitosan–starch composite film: Preparation and characterization. *Industrial Crops and Products*, *21*, 185–192.

Yang, F., Zhang, B., & Ma, Q. (2010). Study of sticky rice–lime mortar technology for the restoration of historical masonry construction. *Accounts of Chemical Research*, *43*, 936–944.

Yu, Q., Xu, J., & Han, Y. (2011). Synthesis and properties control of fluorinated organic–inorganic hybrid films. *Applied Surface Science*, *258*, 1412–1416.

Yuan, S., Pehkonen, S. O., Liang, B., Ting, Y. P., Neoh, K. G., & Kang, E. T. (2011). Superhydrophobic fluoropolymer-modified copper surface via surface graft polymerisation for corrosion protection. *Corrosion Science*, *53*, 2738–2747.

Zheng, W., He, L., Liang, J., Chang, G., & Wang, N. (2011). Preparation and properties of core–shell nanosilica/poly(methyl methacrylate-butylacrylate-2,2,2-trifluoroethyl methacrylate) latex. *Journal of Applied Polymer Science*, *120*, 1152–1161.